Drift and mass spectroscopic studies on the reactivity of rhodium clusters at the surface of polycrystalline oxides

ARTICLE *in* THE JOURNAL OF PHYSICAL CHEMISTRY · NOVEMBER 1992

Impact Factor: 2.78 · DOI: 10.1021/j100202a068

3 AUTHORS, INCLUDING:

Luca Basini

Research Center for Non Conventional Energy

39 PUBLICATIONS **863** CITATIONS

SEE PROFILE

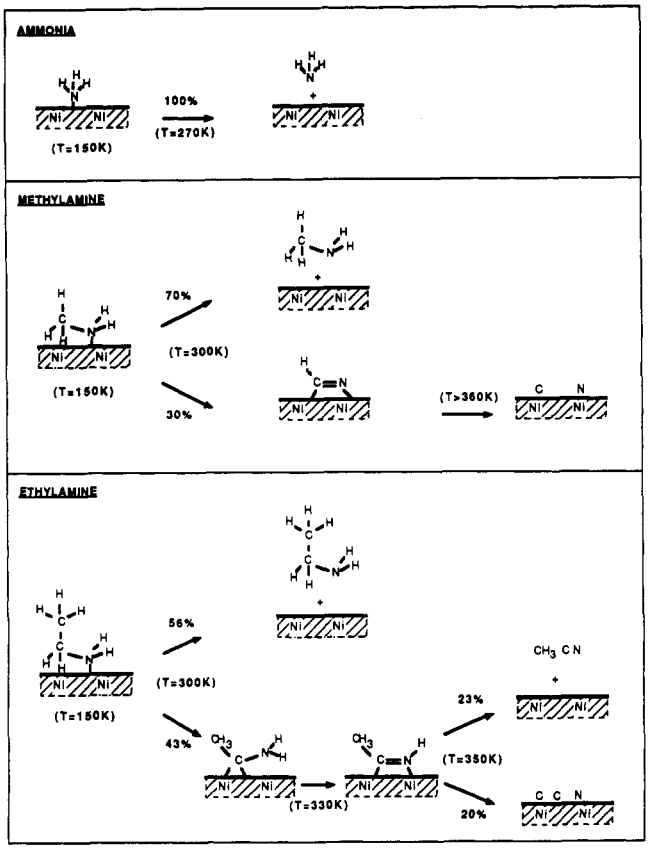

Figure 13. Comparison between ammonia, methylamine, and ethylamine chemistry on Ni(111).

way to that of ethylamine.

Acknowledgment. This work was supported by the Director, Office of Energy Research, Office of Basic Energy Sciences, Material Sciences Division, of the U.S. Department of Energy under Contract DE-AC03-76SF00098. We are also grateful to Rhône-Poulenc for fellowship support (D.G.).

Registry No. CH_3NH_2, 74-89-5; $C_2H_5NH_2$, 7440-02-0; CH_3CN, 75-05-8.

References and Notes

(1) Baca, A. G.; Schulz, M. A.; Shirley, D. A. *J. Chem. Phys.* **1985**, *83*, 6001.
(2) Chorkendorff, I.; Russel, J. N., Jr.; Yates, J. T., Jr. *J. Chem. Phys.* **1985**, *86*, 4692.
(3) Schoofs, G. R.; Benziger, J. B. *J. Phys. Chem.* **1988**, *92*, 741.
(4) Hwang, S. Y.; Seebauer, E. G.; Schmidt, L. D. *Surf. Sci.* **1987**, *188*, 219.
(5) Thomas, P. A.; Masel, R. I. *J. Vac. Sci. Technol.* **1987**, *A5* (4), 1106.
(6) Walker, B. W.; Stair, P. C. *Surf. Sci.* **1981**, *103*, 315.
(7) Pearlstine, K. A.; Friend, C. M. *J. Am. Chem. Soc.* **1986**, *108*, 5842.
(8) Hwang, S. Y.; Kong, A. C. F.; Schmidt, L. D. *J. Phys. Chem.* **1989**, *93*, 8327.
(9) Sasaki, T.; Aruga, T.; Kuroda, H.; Iwasawa, Y. *Surf. Sci.* **1991**, *249*, L347.
(10) Pearlstine, K. A.; Friend, C. M. *J. Am. Chem. Soc.* **1986**, *108*, 5837.
(11) Inamura, K.; Inoue, Y.; Ikeda, S.; Kishi, K. *Surf. Sci.* **1985**, *155*, 173.
(12) Mate, C. M. Ph.D. Dissertation, University of California at Berkeley, 1986.
(13) Froitzheim, H.; Ibach, H.; Lehwald, S. *Rev. Sci. Instrum.* **1975**, *46*, 1325.
(14) Tamaga, K.; Tsuboi, M.; Hirakawa, H. *J. Chem. Phys.* **1968**, *48*, 5536.
(15) Watt, G. B.; Hutchinson, B. B.; Klett, D. S. *J. Am. Chem. Soc.* **1967**, *89*, 2007.
(16) Raval, R.; Chesters, M. A. *Surf. Sci.* **1989**, *219*, L505.
(17) Hamada, Y.; et al. *J. Mol. Spectrosc.* **1983**, *102*, 123.
(18) Wolff, H.; Ludwig, H. *J. Chem. Phys.* **1972**, *56*, 5278. Wolff, H.; Wolff, E. *Ber. Bunsen-Ges. Phys. Chem.* **1965**, *69*, 467.
(19) Gland, J. L.; Fisher, G. B.; Mitchell, G. E. *Chem. Phys. Lett.* **1985**, *119*, 89.
(20) Christmann, K.; Schober, O.; Ertl, G.; Neumann, M. *J. Chem. Phys.* **1974**, *60*, 4528.
(21) Madey, T. E.; Houston, J. E.; Seabury, C. W.; Rhodin, T. N. *J. Vac. Sci. Technol.* **1981**, *18*, 476.
(22) Saillard, J. Y.; Hoffmann, R. *J. Am. Chem. Soc.* **1984**, *106*, 2006.
(23) Kordesch, M. E.; Stenzel, W.; Conrad, H. *Surf. Sci.* **1987**, *186*, 601.
(24) Kordesch, M. E.; Stenzel, W.; Conrad, H. *Surf. Sci.* **1986**, *175*, L687.
(25) Sexton, B. A.; Avery, N. R. *Surf. Sci.* **1983**, *129*, 21.
(26) Hemminger, J. C.; Muetterties, E. L.; Somorjai, G. A. *J. Am. Chem. Soc.* **1979**, *101*, 7238.
(27) Seabury, C. W.; Rhodin, T. N.; Purtell, R. J.; Merril, R. P. *Surf. Sci.* **1980**, *93*, 117.
(28) Andrews, M. A.; Kaesz, H. D. *J. Am. Chem. Soc.* **1979**, *101*, 7238.
(29) Dawoodi, Z.; Mays, M. J.; Raithby, P. R. *J. Organomet. Chem.* **1989**, *219*, 103.
(30) Friend, C. M.; Muetterties, E. L.; Gland, J. L. *J. Phys. Chem.* **1981**, *85*, 3256.
(31) *C.R.C. Handbook of Chemistry and Physics*, 72nd ed.; C.R.C. Press: Boca Raton, FL, 1991-1992.
(32) Cox, J. D.; Pilcher, G. *Thermochemistry of Organic and Organometallic Compounds*; Academic Press: New York, 1970.
(33) To be published.

Drift and Mass Spectroscopic Studies on the Reactivity of Rhodium Clusters at the Surface of Polycrystalline Oxides

Luca Basini,* Mario Marchionna, and Aldo Aragno

Research Division, Snamprogetti S.p.A., Via Maritano 26, I-20097 San Donato Milanese, Milan, Italy
(Received: May 14, 1992; In Final Form: July 8, 1992)

This work presents the results of a systematic experimental study on the chemistry of rhodium clusters on the surfaces of polycrystalline MgO, Al_2O_3, and CeO_2. The reactions were induced by temperature and by reductive and oxidizing treatments followed by interactions with gaseous CO- or CO_2-containing atmospheres. Eight reactivity experiments were performed on each sample in a high-pressure micro-plug-flow reactor and the reactions were followed by DRIFT and mass spectrometry. New findings were made on (a) the formation and reactivity of carbon-containing and oxygen-containing species and of hydridocarbonyl clusters; (b) the influence of the support in determining the chemistry of the rhodium complexes; (c) the differences between the carbonyl surface clusters formed during the CO and the CO_2 hydrogenation reactions; and (d) the balance between temperature and ligand effects in determining the formation of rhodium clusters.

Introduction

The coordinative unsaturations produced on defect sites (steps, kinks, and edges) of crystalline materials and the reactivity of the surface OH groups are responsible for the richness and variety of the chemistry of noble metal complexes on polycrystalline oxides.[1] However, the anisoptropies of the molecular environments are also responsible for the difficulties in achieving structural information on the species generated at the surfaces. Moreover, due to the many different metal cluster species that can be interconverted into one another, the existence of a well-defined

* To whom correspondence should be addressed.

0022-3654/92/2096-9431$03.00/0

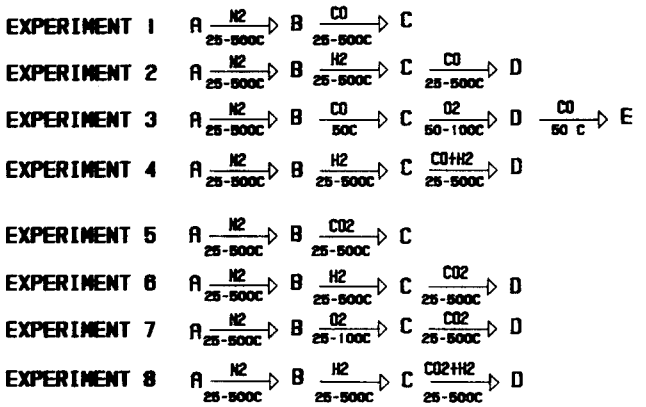

Figure 1. Scheme of the experimental sequences.

species depends on a delicate balance between thermodynamic and kinetic factors.[2] For these reasons, comparisons between the results of different experiments, in which many poorly defined surface structures are produced (as in the case of many heterogeneous catalytic reactions), can be rigorously made only when the experiments are performed on the same material and when the thermodynamic and kinetic experimental parameters are well-defined.

This work discusses and compares the results of eight reactivity experiments performed to investigate the chemistry of rhodium complexes at the surfaces of polycrystalline MgO, Al_2O_3, and CeO_2. The oxides used were highly crystalline and low surface area materials (surface areas below 10 m^2/g), and the rhodium species (0.1% wt/wt) were grafted on them through a chemical reaction between $Rh_4(CO)_{12}$ and the active surface sites. The experimental sequences (Figure 1) have been defined and optimized in order to achieve information that could be cross-compared and analyzed. DRIFT (diffuse reflectance infrared Fourier transform) spectra of the surface species and mass spectra of the reaction products were obtained during the experiments at temperatures between 25 and 500 °C and at a pressure of 0.1 MPa. The reactivity of the reduced and oxidized rhodium surface species with CO and CO_2 has been examined in experiments 1–3 and in experiments 5–7, respectively. The results are useful for discussing the CO hydrogenation (experiment 4) and the CO_2 hydrogenation (experiment 8) reactions. The systematic approach that we have followed reveals some new aspects and confirms other aspects of the rhodium species chemistry under conditions that have not been previously investigated.

Experimental Section

DRIFT Spectra and Mass Spectroscopic Analysis. The spectroscopic experiments were performed with a Nicolet 20SXC spectrometer equipped with a MCT detector (resolution of 4 cm^{-1}). DRIFT spectra of polycrystalline samples were obtained at temperatures between 50 and 500 °C in He, H_2, D_2, O_2, CO, CO_2, CO + H_2, and CO_2 + H_2 flowing gaseous environments at a pressure of 0.1 MPa. In some experiments the purity of the H_2, D_2, and He streams was critical. For this reason very high purity gases (SIAD, electronic grade) were used and were further purified with OMI-1 filters (Supelco, Li and Co compounds supported on resins). The absence of O_2, H_2O, CO, or CO_2 contaminants was checked by mass spectrometry. The DRIFT cell (Spectra-Tech) has all the main features of a micro-plug-flow reactor, and its experimental features have been described in previous works.[3] The powdered polycrystalline materials were placed inside the cell onto a fritted tungsten disk that could be heated up to 900 °C and that permitted flow of the gaseous atmospheres through the samples. Two water-cooled ZnSe windows allowed the incident radiation to reach the powdered samples and the diffuse reflected radiation to be collected into the MCT detector. Light absorption phenomena in the gaseous phases were modeled with the Lambert–Beer equations, while those at the surface of the powdered samples were modeled by means of Kubelka–Munk equations.[4] The cell and the FTIR spectrometer were maintained in a nitrogen-filled drybox that allowed the insertion of the rhodium-containing samples in an inert atmosphere. The cell output line was linked, through a two-orifice sampling system with differential pumping between the orifices, to a quadrupole mass spectrometer (UTI 1-300 amu) equipped with software for selected peak monitoring over time.

Sample Preparation. MgO (99.99% wt/wt) and Al_2O_3 (99.999% wt/wt) were supplied by Aldrich and CeO_2 (99.99% wt/wt) was supplied by Johnson Matthey. All the oxides were purchased stored under He atmosphere. Their purities were checked by optical emission arc spectroscopy. The XRD analysis revealed that the samples were highly crystalline, with a periclase structure (cubic crystals, space group *Fm3m*) in the case of MgO, a corundum structure (ditrigonal structure, space group Pn_2/mnm) in the case of Al_2O_3, and a cerianite structure (cubic crystals, space group *Fm3m*) in the case of CeO_2. The surface areas, measured according to the BET method, were always below 10 m^2/g. The oxides were employed in a moisture-free and CO_2-free environment and were mildly dehydrated (500 °C in a helium flow) before their use; neither the XRD diffraction patterns nor the surface areas were modified after this treatment. The rhodium-containing samples (0.1% wt/wt) were prepared at room temperature in a CO atmosphere by dropping a red *n*-hexane solution of $Rh_4(CO)_{12}$ (prepared according to the method described in ref 5) into a slurry of the powdered oxides in the same solvent. Reaction with the oxide surfaces caused an immediate decoloration of the red cluster solution. After some hours, the solid was isolated by filtration and dried under vacuum at room temperature. The DRIFT spectra of the freshly prepared powdered samples revealed carbonyl absorption bands at 2085 and at 2008 cm^{-1} for the Rh/MgO sample and at 2090 and 2010 cm^{-1} for the Rh/Al_2O_3 sample. These bands are assigned to $Rh(I)(CO)_2$ surface species[6,7] (hereafter referred to as species **1**) formed through an oxidative disaggregation of the rhodium cluster in which the OH groups at the surface of the polycrystalline oxides are involved. This reaction has been described according to eq 1 in refs 6 and 7.

$$Rh_4(CO)_{12} + [M]\text{–}OH \rightarrow [M]\text{–}O\text{–}Rh^{I}(CO)_2 + H_2 + CO \quad (1)$$

Peaks at 2095 and 2010 cm^{-1} assigned to species **1** and a shoulder near 2110 cm^{-1} assigned to a carbonyl complex with rhodium atoms in an oxidation state higher than $+I$[11] were found in the IR spectra of the freshly prepared Rh/CeO_2 sample.

Results

The first step in each of the experiments 1–8 was a thermal treatment of the rhodium-containing samples up to 500 °C in the helium flowing environment (He flow rate, 30 mL/min; heating rate from 25 to 500 °C, 30 °C/min; time of heating at 500 °C, 15 min). This initial treatment was performed in order to gain information on the temperature-induced reactions in inert atmosphere, to condition the materials at high temperature and to obtain the same surface features at the beginning of each experiment.

At increasing temperatures the DRIFT spectra of the three samples (Rh/MgO, Rh/Al_2O_3, Rh/CeO_2) showed the following features: (i) the doublet assigned to species **1** gradually diminished in intensity and at the same time infrared bands assigned to linear- and bridge-bonded CO were formed (Figure 2); (ii) at temperatures higher than 400 °C all the CO stretching bands disappeared; (iii) the stretching bands of the OH groups of the support were strongly reduced (Figure 3). The intensity reduction of the OH stretching bands was not due to the dehydration reactions of the support, since the heating of the pure oxides following the same procedure as for the rhodium-containing oxides did not produce the same modifications in the OH stretching bands. Figure 3 shows the difference spectra obtained by subtraction of the absorption bands of the pure oxides from those of the rhodium-containing oxides. Negative bands at 3652, 3625, and 3315 cm^{-1} for the CeO_2-containing materials (Figure 3A), at 3698, 3615, and 3425 cm^{-1} for the Al_2O_3-containing materials (Figure 3B), and at 3742, 3583, 3784 cm^{-1} for the MgO-containing

TABLE I: Carbonyl Stretching Band Maxima Revealed during Experiment 1 after the CO Pulses in a Helium Flowing Environment

	ν_{CO} (cm^{-1})							
	Rh/MgO			Rh/Al_2O_3			Rh/CeO_2	
T (°C)	geminal	linear	bridged	geminal	linear	bridged	geminal	linear
50	2090 (w) 2015 (w)	1950	1800	2100	2075	1860	2090, 2015	2055
100	2088, 2010	1950 (sh)		2100 2025 (sh)	2060, 2035		2090, 2020	2055 (vw)
200		2037, 2020, 1950 (sh)	1730	2100 (vw)	2045	1860	2093, 2020	
300		2015, 1940 (sh)	1720		2040		2085, 2015	2042
400		2000 1930 (sh)			2010			
500		1980						

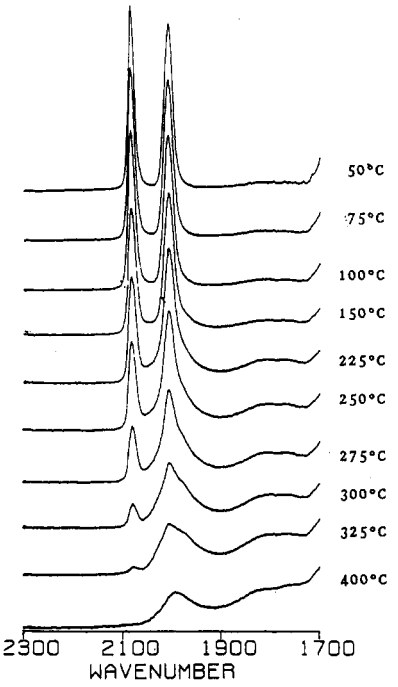

Figure 2. Modifications of the carbonyl stretching bands of Rh/Al_2O_3 induced by the thermal treatment in a helium flow performed in the first step of experiment 1–8.

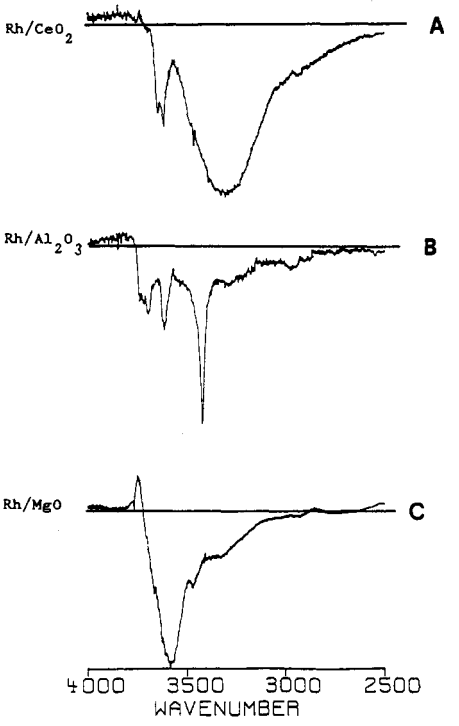

Figure 3. Difference spectra in the OH stretching region, obtained by subtraction of the spectra of the pure oxides from the spectra of the rhodium-containing oxides (both the spectra were recorded at 50 °C after heating at 500 °C in a flowing helium environment): (A) difference spectrum ($Rh/CeO_2 - CeO_2$), (B) difference spectrum ($Rh/Al_2O_3 - Al_2O_3$), (C) difference spectrum (Rh/MgO - MgO).

materials (Figure 3C) were revealed.

The mass spectra recorded during the heating of the three rhodium-containing samples revealed the desorption of CO_2 and CO at temperatures between 100 and 450 °C.

Experiment 1. The samples heated at 500 °C in a helium flow, were cooled to 50 °C and then treated at 50, 100, 200, 300, 400, and 500 °C with a 60-s CO gaseous pulse (CO flow rate, 20 mL/min). The DRIFT spectra of Rh/CeO_2 recorded after the first CO pulse at 50 °C revealed strong peaks assigned to species 1 and a weak band assigned to linear bonded CO. Moreover, a band at 2150 cm^{-1} assigned to carbonyl groups bonded to surface Ce^{IV} ions was also observed. The absorptions of linear- and bridge-bonded CO groups were instead the prevailing features in the IR spectra of Rh/MgO, and the spectra of Rh/Al_2O_3 in which weak absorptions of species 1 were also present (Table I). A second CO pulse at 100 °C resulted in the disappearance of all absorption bands different from those of species 1 from the spectra of Rh/CeO_2. The spectra of Rh/MgO and Rh/Al_2O_3 recorded after the CO pulse at 100 °C showed (i) an intensity increase of the species 1 bands; (ii) a reduction of the linear-bonded CO band intensities; (iii) an almost complete disappearance of the bridge-bonded CO bands (Figure 4 and Table I). At higher temperatures the reaggregation of the rhodium atoms was revealed by the disappearance of the carbonyl bands assigned to species 1 and by the formation of new linear- and bridge-bonded CO species. The complete disappearance of the species 1 absorption bands occurred at different temperatures for the three samples: (i) at 200 °C on Rh/MgO, (ii) at 300 °C on Rh/Al_2O_3; (iii) at 400 °C on Rh/CeO_2 (see Table I). DRIFT spectra were also recorded during the CO gaseous pulses. At each temperature investigated CO stretching bands assigned to linear-bonded CO species (in the frequency range 2030–2065 cm^{-1}) were formed. These bands disappeared in a flowing helium environment (Figure 4).

Experiment 2. The samples were heated at 500 °C in a helium flow, then cooled at 50 °C, and heated again in a hydrogen flow up to 500 °C (H_2 flow rate 30 mL/min; heating rate from 25 to 500 °C, 30 °C/min; time of heating at 500 °C, 15 min). CO gaseous pulses were then introduced into the DRIFT cell at 50, 100, 200, 300, 400, and 500 °C following the same procedure as in experiment 1. The spectra of Rh/MgO and Rh/Al_2O_3 recorded between 50 and 300 °C in a hydrogen flowing environment contained weak peaks in the 1900–2050-cm^{-1} range (Figure 5A). These peaks disappeared at temperatures above 300 °C. A second thermal treatment in a hydrogen flow did not produce any new absorption bands. To exclude that these peaks could be due to rhodium–hydride stretchings,[9] the experimental sequence was repeated on the freshly prepared Rh/MgO, using deuterium instead of hydrogen. In this case the peak formation was observed between 100 and 300 °C. The bands had the same shape as under hydrogen flow, but were downward shifted of 8 cm^{-1} (Figure 5A).

In the third experimental step, the recarbonylation reactions of the reduced samples were studied. The examination of the spectra recorded after the CO pulses on the Rh/CeO_2 sample

TABLE II: Carbonyl Stretching Band Maxima Revealed during Experiment 2 after the CO Pulses in a Helium Flowing Environment

	ν_{CO} (cm^{-1})							
	Rh/MgO			Rh/Al_2O_3			Rh/CeO_2	
T (°C)	geminal	linear	bridged	geminal	linear	bridged	geminal	linear
50		2050	1800		2060	1860	2088, 2015	2055
100	2090 (vw)	2043	1780	2095 (w)	2055, 2030	1860	2090, 2020	2055 (sh)
200		2027	1750		2045	1860	2090, 2015	
300		2014	1720		2035		2080, 2010	2040
		1940 (sh)						
400		2000			2010			
500		1980						

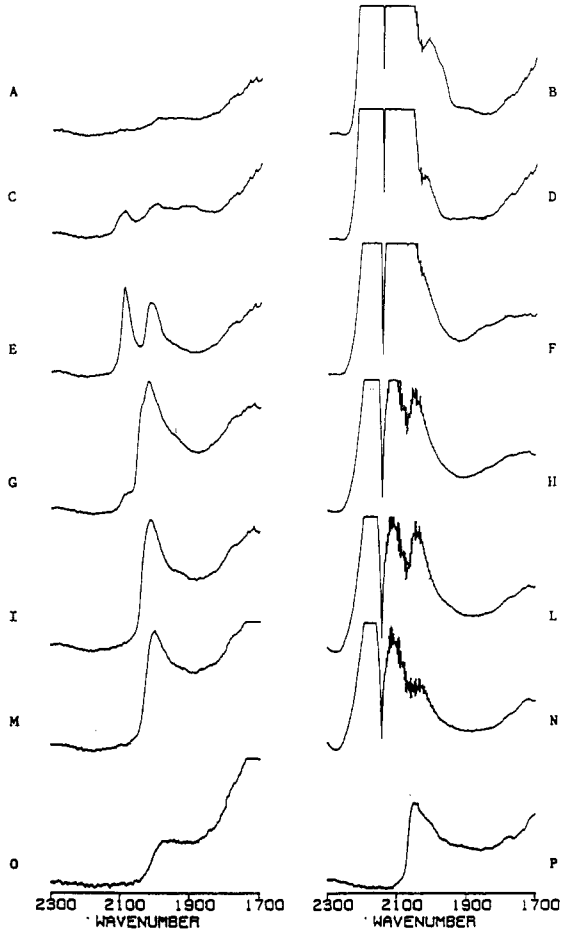

Figure 4. Carbonyl stretching bands produced during experiment 1 on the Rh/MgO sample: (A) spectrum recorded at 50 °C after the thermal treatment at 500 °C in a helium flow; (B, D, F, M, L, N) spectra recorded during the CO pulses respectively at 50, 100, 200, 300, 400, and 500 °C; (C, E, G, I, M, O) spectra recorded after the CO pulses respectively at 50, 100, 200, 300, 400, and 500 °C; (P) spectrum recorded after cooling at 50 °C in a helium flow.

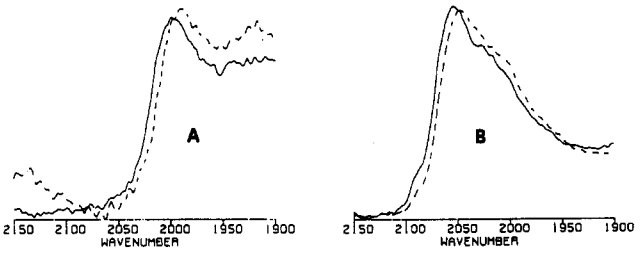

Figure 5. (A) Carbonyl bands formed at 300 °C in the second step of experiment 2 in a hydrogen (continuous line) and a deuterium (dotted line) flow; (B) spectra obtained in the third step of experiment 2 at 50 °C after the interaction with a CO pulse of the hydrogen-treated (continuous line) and deuterium-treated (dotted line) samples.

showed that the rhodium species reactivity toward the gaseous CO was not significantly changed by the hydrogenation treatment (Tables I and II) while the bands assigned to CO molecules bonded

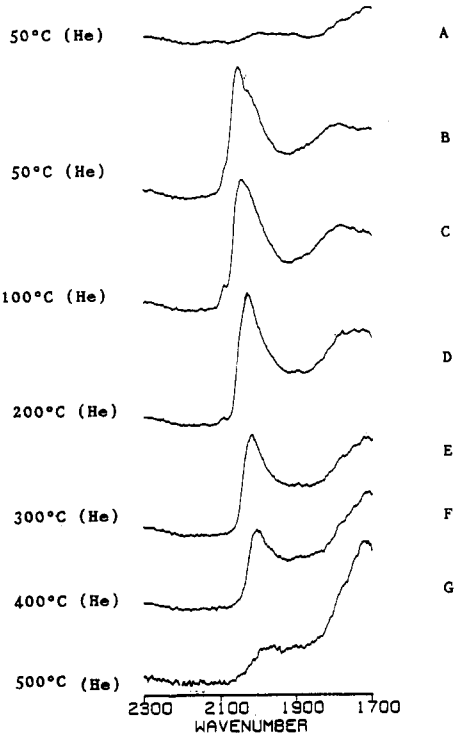

Figure 6. Spectra obtained in experiment 2 after the CO pulses at temperatures between 50 and 500 °C.

to cerium atoms were shifted from 2150 to 2130 cm^{-1}. The CO pulses at 50 and 100 °C did not produce the disaggregation of the rhodium clusters formed after the hydrogenation of Rh/MgO and Rh/Al_2O_3; shoulders assigned to geminal-bonded CO groups and strong bands assigned to linear- and bridge-bonded CO were revealed at these temperatures (Figure 6). At 200 °C the weak bands assigned to species 1 disappeared completely in the spectra of Rh/MgO while they were still distinguishable in the spectra of Rh/Al_2O_3. In both cases the linear-bonded CO species were the prevailing features of the spectra. At higher temperatures the same bands observed during experiment 1 were again revealed (Tables I and II and Figures 4 and 6).

The recarbonylation reactions were also studied on the Rh/MgO sample which was reduced in a deuterium flowing environment. The spectra obtained at 50 100 and 200 °C after interaction with the gaseous CO pulses showed some peaks assigned to linear- and bridge-bonded CO species with the same shape and multiplicity as the signals revealed on the H_2-treated samples. Again, the peak maxima assigned to the linear-bonded CO species were downward shifted by 8 cm^{-1} (Figure 5B).

Experiment 3. The samples were heated in a helium flow at 500 °C and recarbonylated at 50 °C with a 10-s CO pulse (CO flow rate 20 mL/min; see Figure 7). Subsequently, an oxygen flow was introduced into the cell (oxygen flow rate, 10 mL/min) and the temperature was increased to 100 °C. The interaction with oxygen produced (i) the disappearance of the IR bands assigned to linear and bridge CO species (Figure 7, C and C'), (ii) an increase in intensity of the doublets assigned to the geminal carbonyl complexes and, at 100 °C on Rh/CeO_2, the formation of a singlet at 2110 cm^{-1} assigned to CO groups bonded to rhodium

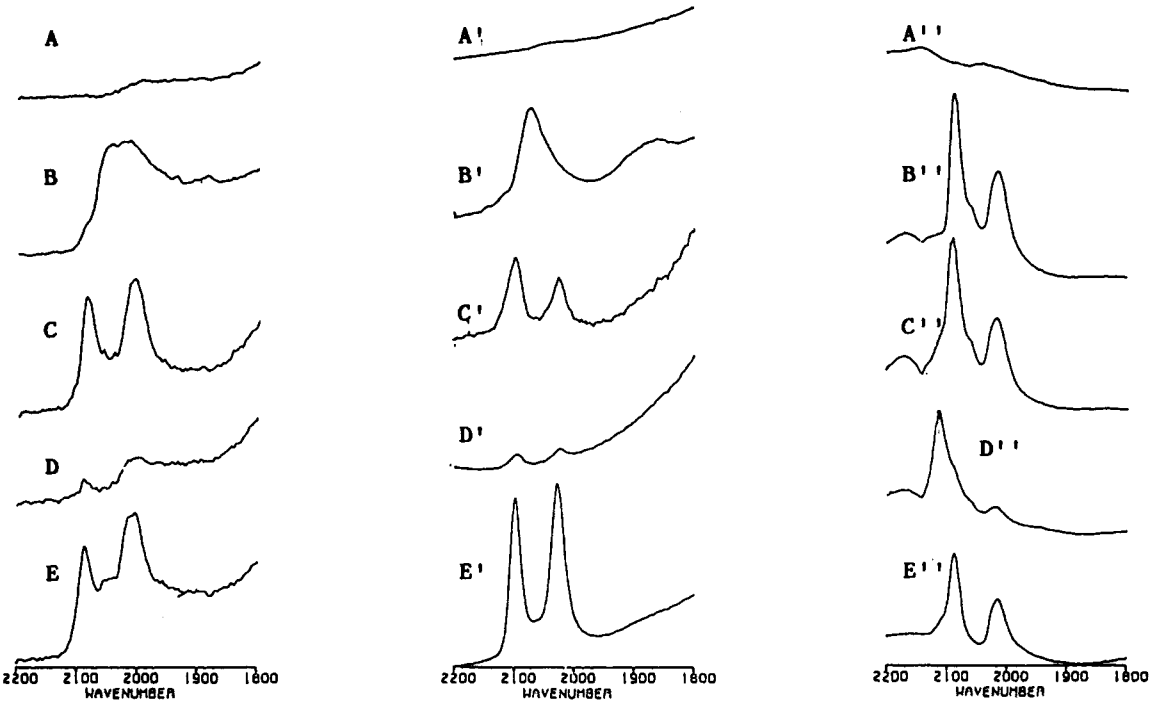

Figure 7. Spectral sequences recorded during experiment 3 in the oxidative decarbonylation reactions of Rh/MgO, Rh/Al_2O_3, and Rh/CeO_2. (A, A′, A″) spectra of the samples after the heating in helium; (B, B′, B″) spectra of the samples recarbonylated with a 1-min CO pulse; (C, C′, C″) spectra of the recarbonylated samples recorded at 50 °C in flowing oxygen; (D, D′, D″) spectra of the recarbonylated samples in an oxygen flow at 100 °C; (E, E′) spectra recorded in helium at 50 °C after a second CO pulse; (E″) spectrum recorded at 50 °C in a hydrogen flow after the oxidizing treatment.

TABLE III: Carbonyl Stretching Band Maxima Revealed during Experiment 4 in CO + H_2 and He Flowing Environments

	ν_{CO} (cm^{-1})					
	Rh/MgO		Rh/Al_2O_3		Rh/CeO_2	
T (°C)	CO + H_2	He	CO + H_2	He	CO + H_2	He
50	2088, 2057, 2016, 1800	2086, 2052, 2014, 1800	2068, 2025, 1860	2090, 2050, 2035, 1860	2085, 2050, 2014	2085, 2050, 2013
100	2090, 2051, 2020, 1800	2090, 2043, 2020, 1800	2061, 2030, 1860	2091, 2042, 2030, 1860	2083, 2054, 2010	2083, 2052, 2010
200	2035, 1800	2020, 1780	2048, 1860	2038, 1860	2086, 2014	2086, 2014
300	2030, 1770	2010, 1750	2046	2030	2085, 2050, 2015	2032
400	2025, 1740	1990, 1720	2041	2020	2035	2000
500	2020, 1970, 1700	1970, 1700	2030		2010 (vw)	

atoms in a higher oxidation state[11] (Figure 7D″); (iii) the formation of CO_2 (detected by mass spectroscopy) in the output line. After heating for 30 min in an oxygen flow, the carbonyl stretching bands almost disappeared in the spectra of Rh/MgO and Rh/Al_2O_3 (Figure 7, D and D′), while the peak at 2110 cm^{-1} was still distinguishable in the spectra of Rh/CeO_2. By treating the oxidized Rh/CeO_2 at 100 °C with a gaseous hydrogen pulse, species **1** was again formed together with a broad absorption band near 3600 cm^{-1} while the peak at 2110 cm^{-1} disappeared (Figure 7E″). Species **1** was also produced, together with gaseous CO_2, on oxidized Rh/MgO and Rh/Al_2O_3 after interaction with a gaseous CO pulse (Figure 7, E and E′).

Experiment 4. The surface reactivity with the CO + H_2 mixture (flow rate, 20 mL/min; H_2/CO = 2 vol/vol) at 50, 100, 200, 300, 400, and 500 °C was studied with samples previously heated at 500 °C in flowing helium and in flowing hydrogen following the procedure described for experiment 2 (during the heating in hydrogen flow the samples gave the same IR bands in the 1900–2050-cm^{-1} range, as described above). DRIFT spectra were collected, at each temperature investigated, before, during, and after the 10-min interaction with the CO + H_2 mixture.

The only difference between the spectra obtained during experiments 2 and 4 at 50 and 100 °C was the formation of resolved peaks, instead of weak shoulders, at 2090 and 2015 cm^{-1} (assignable to species **1**) in the 50 °C spectrum of Rh/MgO (Figures 6 and 8). Only at higher temperatures did the presence of hydrogen have a detectable influence on the position and intensity of the carbonyl stretching bands of each sample. At 200, 300, 400, and 500 °C it was observed that the peaks assigned to linear-bonded CO were in most cases downward shifted by 5–10 cm^{-1} as compared with the ones produced in experiments 2 (Tables II and III and Figures 6, 8, 9, and 10). The spectra of Rh/CeO_2 showed the doublet assigned to species **1** both in flowing CO + H_2 and in helium atmosphere up to 200 °C. The peak maxima assigned to species **1** were not shifted by replacing the syn-gas mixture with helium (Table III and Figure 10).

The maxima of the carbonyl bands present in the spectra under flowing CO + H_2 atmosphere and subsequently under helium atmosphere are compared in Table III. An upward frequency shift of the linear- and bridge-bonded CO species bands (10 and 20 cm^{-1}) was always observed in flowing CO + H_2 environment.

The mass spectroscopic analysis performed on the output stream during the interaction with the CO + H_2 atmosphere showed that (i) the CO hydrogenation reaction did not occur on Rh/CeO_2 when species **1** was the only surface carbonyl species detected in the DRIFT spectra; (ii) CH_4, H_2O, and CO_2 were produced contemporaneously during the hydrogenation reaction.

Experiment 5. The samples were heated in a helium flow up to 500 °C and, after cooling, were treated at 50, 100, 200, 300, 400, and 500 °C with 3-min gaseous pulses of pure CO_2 (flow rate 20 mL/min). Very weak and broad absorption bands, assigned to linear-bonded CO species, were revealed only at temperatures higher than 400 °C under flowing CO_2 and quickly disappeared under a helium flow. The mass spectroscopic analysis performed by subtracting the spectrum of pure CO_2 from the mass spectra of the cell output streams revealed the formation of CO at the temperatures at which the weak carbonyl stretching bands were also present. The samples cooled to 50 °C were also treated with a CO pulse. Surface complexes were formed with CO stretching bands assigned to geminal, linear-bonded, and

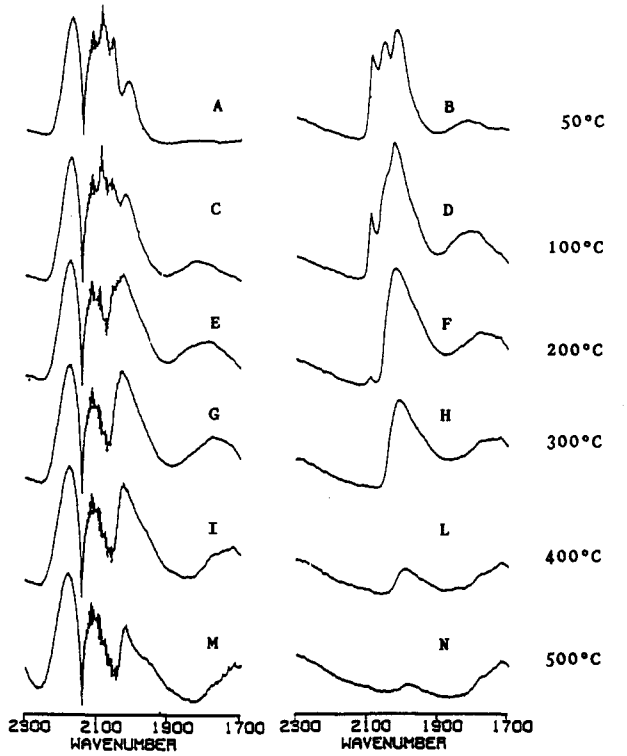

Figure 8. Spectra obtained in experiment 4 between 50 and 500 °C on Rh/MgO during (A, C, E, G, I, M) and after (B, D, F, H, L, N) the 10-min CO + H_2 pulses.

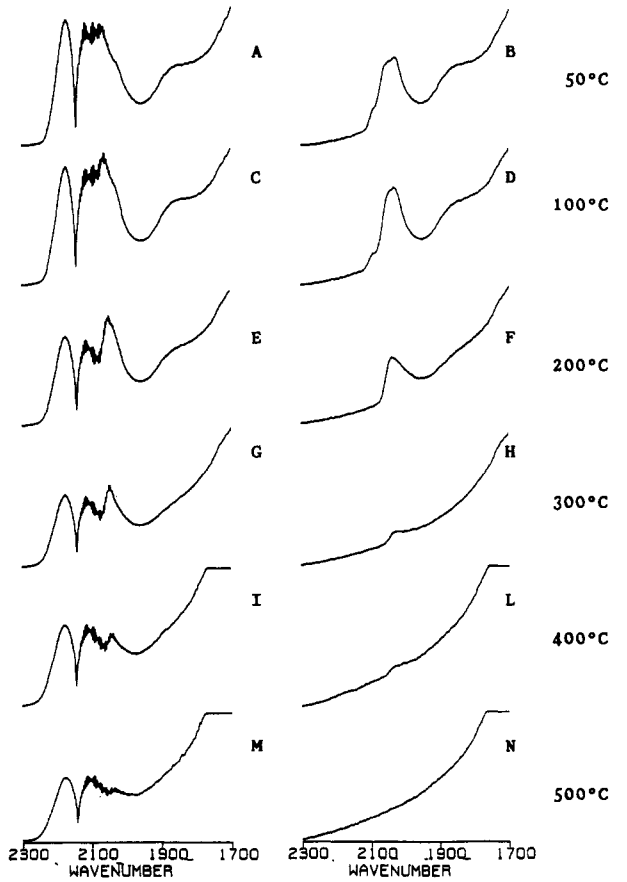

Figure 9. Spectra obtained in experiment 4 between 50 and 500 °C on Rh/Al_2O_3 during (A, C, E, G, I, M) and after (B, D, F, H, L, N) the 10-min CO + H_2 pulses.

bridge-bonded CO on Rh/MgO and Rh/Al_2O_3, while on Rh/CeO_2 only geminal- and linear-bonded CO were revealed. The formation of gaseous CO_2 was also detected during the recarbonylation reactions.

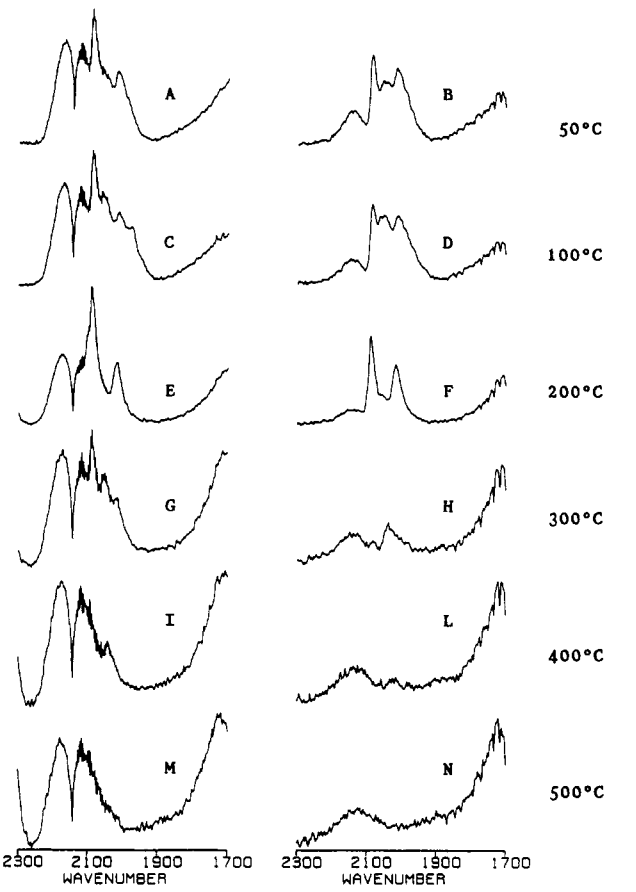

Figure 10. Spectra obtained in experiment 4 between 50 and 500 °C on Rh/CeO_2 during (A, C, E, G, I, M) and after (B, D, F, H, L, N) the 10-min CO + H_2 pulses.

TABLE IV: Carbonyl Stretching Band Maxima Revealed in Experiment 6 in a Flowing CO_2 Environment

	ν_{CO} (cm^{-1})		
T (°C)	Rh/MgO	Rh/Al_2O_3	Rh/CeO_2
50	2025		
100	2030		
200	2024	2050, 2030	2015
300	2020	2040	2000
400	2010	2030	1990
500	1985		1980

Experiment 6. The samples were first heated in helium and then in a hydrogen flow with the same procedure as in experiment 2 (carbonyl bands were again evident during the heating in hydrogen as described in experiments 2 and 4). After cooling, CO_2 pulses were introduced into the DRIFT cell at 50, 100, 200, 300, 400, and 500 °C. Carbonyl bands were revealed both during and after the CO_2 pulse. The bands appeared at 50 °C on Rh/MgO, above 100 °C on Rh/Al_2O_3, and above 200 °C on Rh/CeO_2 (Table IV and Figure 11). The spectra recorded on Rh/MgO revealed that (i) between 100 and 300 °C the peaks increased in intensity, sharpened, and were downward shifted with increasing temperatures, and (ii) at 400 and 500 °C the bands were reduced in intensity and broadened. The evolution of the carbonyl stretching bands of the Rh/Al_2O_3 and Rh/CeO_2 samples followed the same pattern in the temperature range between 200 and 300 °C.

The experimental sequences were repeated on Rh/Al_2O_3 using deuterium instead of hydrogen. In this case the formation of a carbonyl band was first observed at 300 °C (instead of 200 °C) in a flowing CO_2 environment and the peak maximum (2015 cm^{-1}) was downward shifted by 8 cm^{-1}. The mass spectroscopic analysis of the output line, performed during the CO_2 pulses, revealed the formation of CO at the temperatures at which the carbonyl stretching bands appeared. The DRIFT spectra of the cooled

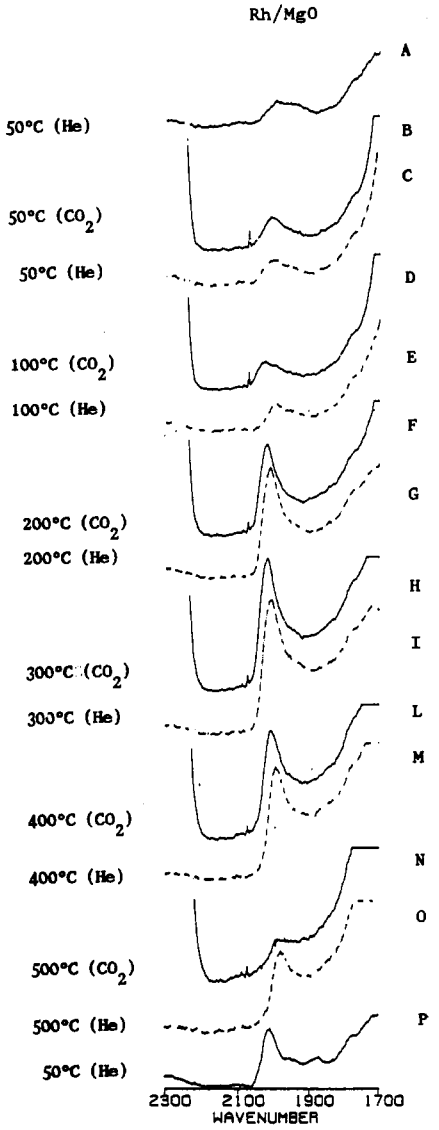

Figure 11. Spectra recorded in experiment 6 during (continuous line, spectra B, D, F, H, L, N) and after (dotted line, spectra C, E, G, I, M, O) the interaction between gaseous CO_2 and Rh/MgO. At point A is reported the spectra of the sample before the interaction with CO_2; at point P is reported the spectra recorded after cooling.

samples at the end of the experiment still showed carbonyl absorption bands assigned to linear-bonded CO. Treatment of the cooled samples with a gaseous CO pulse produced peaks assigned to geminal, linear-bonded CO species on Rh/MgO and Rh/Al_2O_3, while only geminal-bonded CO species were revealed on Rh/CeO_2. During the CO pulses the formation of a small amount of CO_2 was revealed by mass spectroscopy.

Experiment 7. The samples were heated in a helium flow, cooled at 50 °C and heated again in an oxygen flow at 100 °C for 30 min (oxygen flow rate 10 mL/min). Pulses of CO_2 were then introduced into the DRIFT cell at 50, 100, 200, 300, 400, and 500 °C. The interaction of oxidized Rh/CeO_2 with CO_2 pulses did not produce any carbonyl bands in the DRIFT spectra. However, carbonyl bands were present on Rh/Al_2O_3 at 200, 300, 400, and 500 °C after having switched the CO_2 stream with helium (Figure 12 and Table V). These bands disappeared when CO_2 was reintroduced into the cell. This effect was found also for Rh/MgO, but in this case the carbonyl bands (observed in the helium flow) were strongly reduced in intensity and did not completely disappear in a CO_2 atmosphere. The mass spectroscopic analysis of the output stream during the pulses revealed the formation of CO. The spectra recorded at 50 °C, after cooling in He flow, did not always reveal surface carbonyl complexes. A CO gaseous pulse on the cooled samples produced gaseous CO_2 and IR bands assigned to geminal- and linear-bonded CO species

TABLE V: Carbonyl Stretching Band Maxima Revealed in Experiment 7 after the CO_2 Pulses in a Helium Flowing Stream

	ν_{CO} (cm^{-1})		
T (°C)	Rh/MgO	Rh/Al_2O_3	Rh/CeO_2
50			
100			
200	2002	2020	
300	2006	2025	
400	1986	2005	
500	1969	2000	

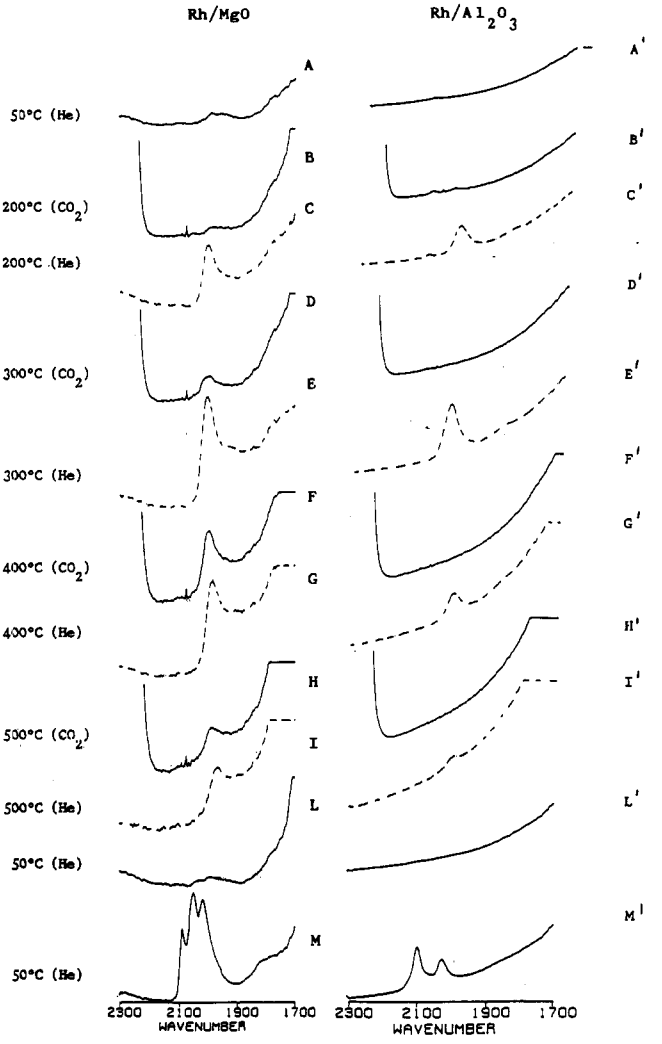

Figure 12. Spectra recorded in experiment 7 during (continuous line) and after (dotted line) the interactions between CO_2 and preoxidized Rh/MgO and Rh/Al_2O_3. The spectra M and M' were recorded in helium flow after a CO pulse at the end of the experiment.

on Rh/MgO, while geminal-bonded species were only detected on Rh/Al_2O_3 and Rh/CeO_2.

Experiment 8. The three samples were heated in a helium flow up to 500 °C and then in hydrogen up to 500 °C as in experiments 2, 4, and 6. In a third step, 10-min gaseous pulses of $CO_2 + H_2$ (H_2/CO_2 = 3/1 vol/vol, flow rate 30 mL/min) were introduced into the cell at 50, 100, 200, 300, 400, and 500 °C. The peak maxima of the DRIFT spectra recorded during and after the $CO_2 + H_2$ pulses are reported in Table VI. When the helium flow replaced the $CO_2 + H_2$ environment, the band intensities were strongly reduced and their maxima were shifted to lower frequency values. Carbonyl bands were found at each temperature investigated for Rh/MgO, while no carbonyl bands were detected at 50 °C for Rh/Al_2O_3 and Rh/CeO_2 (Figure 13, A, B, and C). Our observations are summarized as follows: (a) no carbonyl bands assigned to species 1 were found for any case investigated; (b) the carbonyl bands were sharpened by increasing the temperature up to 300 °C, while at 400 and 500 °C they were weakened and

TABLE VI: Carbonyl Stretching Band Maxima Revealed in Experiment 8 in $CO_2 + H_2$ and in He Flowing Environments

	ν_{CO} (cm^{-1})					
	Rh/MgO		Rh/Al_2O_3		Rh/CeO_2	
T (°C)	$CO_2 + H_2$	He	$CO_2 + H_2$	He	$CO_2 + H_2$	He
50	2058	2050	2038	2032		
100	2049	2041	2043, 2028	2041, 2023	2052, 2030	2045, 2015
200	2035	2030	2054, 2032	2054, 2030	2050, 2028	2045, 2015
300	2029	2015	2048, 2026	2020	2042	2000 (vw)
400	2021	1990	2020	1990	2010	
500	2015		2010		1980	

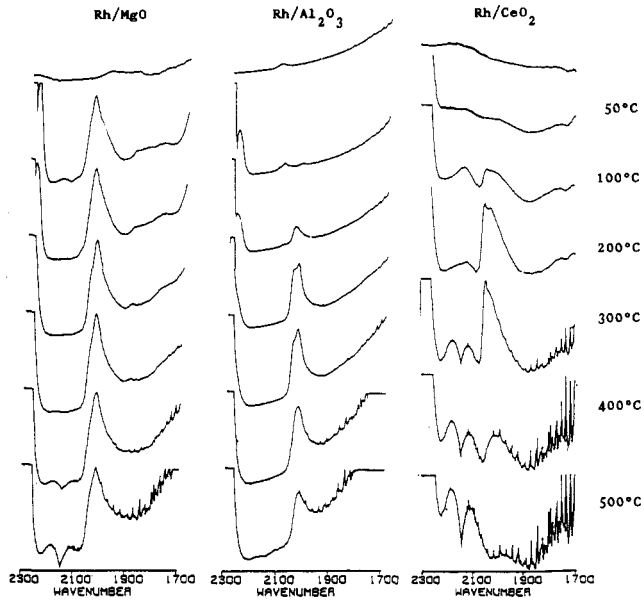

Figure 13. Spectra recorded between 50 and 500 °C on Rh/MgO, Rh/Al_2O_3, and Rh/CeO_2 during the interaction with the $CO_2 + H_2$ mixture (experiment 8).

broadened; (c) the peak maxima resulted monotonically downward shifted at increasing temperatures; (d) absorption bands of formate species (2960, 2855, 1685, 1350 cm^{-1}) were first detected for Rh/MgO and Rh/CeO_2 at 100 °C (at this temperature the formation of CH_4 was not detected) and were stable up to 400 °C; (e) the contemporary formation of H_2O, CO, and CH_4 was detected in the output stream starting from 300 °C.

Discussion

Surface Reactions Induced by Thermal Treatment in Helium and Hydrogen Flows. The DRIFT spectra recorded after the reaction between $Rh_4(CO)_{12}$ and CeO_2 showed, together with the absorption bands assigned to species **1**, a shoulder at 2110 cm^{-1} which is assigned to the formation of an oxidized rhodium carbonyl species. During the heating of the three samples examined the following was observed: (i) the decarbonylative aggregation of species **1** (Figure 2); (ii) a selective reduction of the intensity of some OH stretching bands (Figure 3); (iii) the desorption of CO_2 but not of hydrogen. These three phenomena must be related since the same reduction of the OH stretching band intensities was not observed in the absence of rhodium and the desorption of CO_2 could only originate by the reductive agglomeration of species **1**. These findings strongly support the occurrence of a surface water gas shift (SWGS) reaction (2) in which the formation of hydridocarbonyl species is suggested by the fact that no hydrogen was detected in the output stream. It can also be hypothesized that hydridocarbonyl clusters are formed through the involvement of a back spillover effect which allows the interactions between the rhodium species and the mobile protons of the support.[9]

$$[M]\text{–}O\text{–}Rh(CO)_2 + [M]\text{–}OH \rightarrow [MO_x{\cdot}H_zRh_y(CO)_n] + CO_2 \quad (2)$$

At temperatures higher than 300 °C the hydridocarbonyl complexes are decarbonylated, partially by desorption of CO molecules and partially by dissociation of the C–O bonds to produce carbon-containing species and oxygen-containing species. This last conclusion is inferred by the detection of new carbonyl bands in the spectra of the decarbonylated samples when the helium flow was switched with hydrogen[13] (second step of experiments 2, 4, 6, and 8). The same result was obtained for Rh/MgO with deuterium instead of hydrogen but in this case the carbonyl peaks were downward shifted by 8 cm^{-1}. This finding is consistent with an isotopic shift two bonds removed from the CO group[10] and sustains the assignment of the carbonyl bands to hydrido (deutero) carbonyl clusters. It was also observed that the carbonyl bands first appeared at 200 °C in a deuterium flow. This is interpreted as the occurrence of a kinetic isotopic effect which reduced the formation rate of the deutero carbonyl clusters.

Surface Reactions Induced by Interaction with CO (Experiments 1–3). The rhodium clusters produced on the heating of species **1** in helium were reconstructed with CO pulses to a different extent depending on the temperature and on the support during experiment 1. At 50–100 °C, the 5-min CO pulses have a disaggregative effect on the rhodium clusters since species **1** was the only carbonyl complex detected at the surface of Rh/CeO_2 and was formed together with linear-bonded CO species on the Rh/MgO and Rh/Al_2O_3[8] (Figure 4 and Table I). At higher temperatures species **1** was stabilized only at the surface of CeO_2 which is known to have oxidizing properties due to the mobile lattice–oxygen atoms.[12,16] The complete disaggregation of the clusters on Rh/MgO and Rh/Al_2O_3, to produce at first species **1** and subsequently decarbonylated rhodium species, was obtained at low temperatures (50–100 °C) in a flowing oxygen stream during experiment 3. The same treatment on Rh/CeO_2 transformed species **1** into a more highly oxidized rhodium carbonyl complex (ν_{CO} 2110 cm^{-1}) before complete decarbonylation was achieved (Figure 7D″). In a hydrogen atmosphere this oxidized rhodium carbonyl complex was transformed again into species **1** and surface hydroxyl groups (represented as –OH in eqs 3 and 4). Mass spectrometry revealed the formation of CO_2 during the treatment of the three samples in an oxygen flow. This molecule was also produced, together with species **1**, when the decarbonylated and oxidized samples were treated with CO at room temperature. These reactivity features have already been described in literature[17] and suggest that a rhodium–oxygen adduct $[M]\text{–}O\text{–}Rh(O)_x$ (hereafter referred to as species **2**) remains on the surface after the oxidative decarbonylation and react with CO to give species **1** and CO_2.

$$Rh^I(CO)_2 + O_2 \rightarrow Rh^z(O)_y(CO)_m \quad (3)$$

$$Rh^z(O)_y(CO)_m + H_2 \rightarrow Rh^I(CO)_2 + \text{–OH} \quad (4)$$

The interaction with hydrogen up to 500 °C (second step of experiment 2) inhibits, on Rh/MgO and Rh/Al_2O_3, the low-temperature (50–100 °C) disaggregation reactions induced by CO chemisorption that were recorded during experiment 1. The downward frequency shift of the carbonyl stretching bands, revealed when deuterium is used to reduce Rh/MgO, strongly suggests the formation of hydrido (deutero) carbonyl clusters (Figure 5B). The inhibitive effect of the hydrogen (deuterium) pretreatment toward the low-temperature disaggregation induced by CO chemisorption is not observed on the Rh/CeO_2 sample. However, in this case heating in hydrogen produces a downward frequency shift, from 2150 to 2125 cm^{-1}, of the CO stretchings assigned to carbonyl groups bonded to the cerium atoms. This shows the occurrence of a reduction of the exposed cerium ions from Ce^{IV} to Ce^{III}.[18]

Surface Reactions Induced by Interaction with CO_2 (Experiments 5–7). The promotion of the CO_2 reductive chemisorption reaction obtained after a hydrogen pretreatment was clearly shown by a comparison of the DRIFT spectra recorded during experiments 5 and 6. This effect was previously observed (by chemisorption measurements) both on rhodium single-crystal surfaces[19] and on supported rhodium aggregates.[20,21] In the present work this phenomenon has been studied for the first time with spectroscopic experiments which have revealed that the enhancement of CO_2

chemisorption is related to the formation of hydrido (deutero) carbonyl complexes. In fact, the formation of carbonyl bands was achieved at higher temperatures and lower frequencies (8–10 cm^{-1}) when deuterium was used instead of hydrogen in the reductive pretreatment of the Rh/Al_2O_3 sample. By analogy with the results and the discussion of experiment 2, these findings are interpreted as indicative of the occurrence of a kinetic isotopic effect that reduces the reaction rate of the reductive chemisorption of CO_2 and of the occurrence of an indirect isotopic shift on the carbonyl stretching.[10]

Solymosi et al. have shown that a key step in CO_2 chemisorption on noble metal single crystals (Pt, Pd, Rh) is the partial negative charge transfer from the metal to CO_2.[26] The same authors observed that the activation energy for this process was lowered by reducing the work function of the metal by chemical deposition of potassium. The K-induced activation of CO_2 initially produced surface CO_2^- species which then dissociate, originating CO with different mechanisms at the different temperatures.[26] Other authors reported that the hydrogen chemisorption on metal surfaces has the effect of increasing the noble metal work functions.[27] These facts suggest that the enhancement in the CO_2 reductive chemisorption on hydrogen-treated metal surfaces is directly related to a metal-mediated interaction between the CO_2 and hydride species, and not to an improvement of the electronic properties of the surface metal clusters. Analogies can also be found at the molecular level with the reductive CO_2 insertion reaction in M–H bonds of hydridocarbonyl complexes.[28]

The spectral sequence of Figure 11 shows that the stretching bands of linear-bonded CO are enhanced in intensity, sharpened, and downward shifted at increasing temperatures between 50 and 300 °C. These unusual findings (revealed both during the CO_2 reductive chemisorption in experiment 6 and during the CO_2 hydrogenation reactions in experiment 8) are interpreted by assuming that the CO_2 reductive chemisorption induces a selective rearrangement of the surface metallic structures and produces well-defined clusters. In fact, an intensity increase of the CO stretchings owing to an enhancement in the surface concentration of CO on large rhodium aggregates should be followed by an upward frequency shift promoted by dipole–dipole coupling and by chemical shift effects.[22]

While only linear-bonded CO species were found in experiments 5 and 6 during and after exposure to CO_2, the formation of species **1** (together with linear-bonded CO species on Rh/MgO and Rh/Al_2O_3) and of gaseous CO_2 was induced with a CO pulse at 50 °C at the end of both experiments. These findings show that the CO molecules produced upon the reductive chemisorption of CO_2 are not able to disaggregate the rhodium clusters, while the disaggregation of the clusters was easily achieved in the presence of CO in the gaseous environment.

The formation of gaseous CO_2, observed during the CO pulse which concluded experiment 6, indicates that reactive oxygen species, which have probably spilled over onto the support, are produced during the CO_2 reductive chemisorption reactions.

The reactivity features described up to now are summarized by eq 5, in which the surface oxygen species are represented by O_s.

$$[MO_y]Rh_wH_n + CO_2 \rightarrow [MO_y]Rh_wH_n(CO)_p + O_s \qquad [M = Mg, Al, Ce] \quad (5)$$

Experiment 7 revealed the formation of carbonyl complexes also during the high-temperature interaction of CO_2 with oxygen-treated Rh/MgO and Rh/Al_2O_3 but not with oxygen-treated Rh/CeO_2. Strangely enough, the carbonyl species were stabilized in inert atmosphere but not under flowing CO_2 environment. We tentatively propose (Scheme I) that the species **2** produced in the oxygen flow are aggregated and reduced at increasing temperatures to form rhodium clusters (according to the results of experiment 3) and atomic oxygen species. These clusters could react with CO_2, originating rhodium carbonyl species and, again, atomic oxygen. The balance between the oxidizing and disaggregative properties of the atomic oxygen species together with aggregative effect induced by the increasing temperature, could produce the

SCHEME I

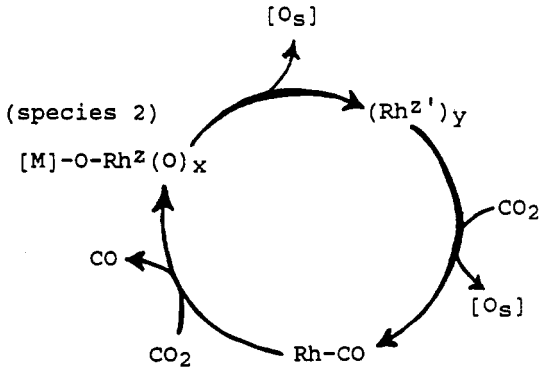

appearance and disappearance of carbonyl bands in the DRIFT spectra. We propose that in the absence of gaseous CO_2 flow the thermal effect prevails, while in the presence of CO_2 the oxidative effect prevails, thus disaggregating the carbonyl clusters and producing species **2** and gaseous CO molecules. The differences in the reactivity features among the different oxide samples could be due to the formation of oxidized rhodium species which are highly stabilized on CeO_2.

Reactivity with CO + H_2 and CO_2 + H_2 Mixtures (Experiments 4 and 8). Results described in the literature on CO and CO_2 methanation reactions have shown that (i) the CO_2 hydrogenation catalyzed at 300 °C by rhodium-containing powdered oxides has a higher selectivity and a higher rate for CH_4 production (by an order of magnitude) as compared with the CO hydrogenation reaction;[23] (ii) the CO methanation rate was found to be inversely proportional to the CO partial pressure,[24] while CO_2 methanation is positively proportional to the CO_2 partial pressure;[25] (iii) both CO and the CO_2 methanation occur through the intermediate formation of carbon-containing species.[14j,25a,b]

A comparison of the DRIFT spectra of experiments 2 (interactions with pure CO pulses) and 4 (interactions with the CO + H_2 mixture) shows that the carbonyl complex formation at 50, 100, and 200 °C is weakly affected by the presence of hydrogen in the CO containing atmosphere (Tables II and III, and Figures 6, 8, 9, and 10). This is sustained by the enhanced formation of species **1** during the 10-min CO + H_2 pulse at 50 °C (Figure 8B) compared with the formation of the same species **1** during the 5-min pure CO pulse (Figure 6B). Carbonyl clusters were, however, formed on Rh/Al_2O_3 and Rh/CeO_2 at lower temperatures in a CO_2 + H_2 flow (experiment 8) than in a pure CO_2 flowing environment (experiment 6). Thus, the presence of surface hydrogen species has a relevant role in carbonyl cluster formation at temperatures below 300 °C only if these are produced through the reductive chemisorption of CO_2. Further, the CO stretching bands in the DRIFT spectra recorded in CO + H_2 and CO_2 + H_2 flowing environments were different in position, shape, and multiplicity (Tables IV and VI and Figures 8, 9, 10, and 13A–C). Broad bands assigned to linear- and bridge-bonded CO species were found together with the absorptions of species **1** under flowing CO + H_2. Under CO_2 + H_2 flow, peaks assigned to linear-bonded CO were sharpened, enhanced in intensity, and downward shifted at increasing temperatures, between 50 and 300 °C. These findings are interpreted by assuming the selective formation of only few kinds of surface clusters during CO_2 methanation,[22] and many different carbonyl species during CO methanation. The formation of species **1** only during the CO hydrogenation experiments at temperatures below 300 °C further indicates that the CO molecules produced during the CO_2 reductive chemisorption reactions were not capable of disaggregating the rhodium clusters.

Carbonyl cluster stretching bands were revealed both during the CO and CO_2 hydrogenation reactions and under an inert atmosphere by substituting the reactants mixture with helium. The two cases differ by a weakening and a downward frequency shift of the bands under helium flow. Recently, Fujita et al.,[14j] by using the transient response[26] and the temperature-programmed

reaction (TPR) methods, revealed the presence of carbon-containing species, oxygen-containing species, and reversibly adsorbed CO molecules on Ni/Al_2O_3 samples. These authors also established that differences in the methanation reaction rates were due to the amount of reversibly chemisorbed CO. By analogy with the work of Fujita, the carbonyl clusters revealed in the DRIFT spectra might be the precursors of both the "carbon-containing" and the "oxygen-containing" intermediate species.

The occurrence of the water gas shift (WGS) reaction and of the reverse water gas shift (RWGS) reaction was revealed, by DRIFT and mass spectroscopy, during the CO and the CO_2 methanations. The "shift" reactions produced (i) CO molecules during CO_2 methanation and (ii) CO_2 molecules during the CO methanation reactions. It could be hypothesized that, if the shift reaction rates are much faster than methanation, then the differences in selectivities and activities of the CO and CO_2 hydrogenation would be reduced. This is not pertinent to the experiments described here, during which different carbonyl stretching bands were revealed during the two reactions.

Conclusions

The experiments described here have revealed a number of new aspects of the chemistry of rhodium carbonyl complexes at the surfaces of polycrystalline oxides, in particular the following.

(a) Investigations of the reductive and aggregative decarbonylation reactions of the $Rh^I(CO)_2$ surface species induced by a thermal treatment up to 500 °C in inert atmosphere have revealed (i) the occurrence of a SWGS reaction which consumes the OH groups of the supports, producing rhodium clusters and gaseous CO_2 (see eq 2); (ii) the breaking of the C–O bonds of some carbonyl groups and the formation of carbon- and oxygen-containing rhodium clusters which, by further heating in a flowing hydrogen (deuterium) stream, were transformed into hydrido (deutero) carbonyl clusters (experiments 2, 4, 6, and 8).

(b) The enhancement of the CO_2 chemisorption reactions, which follows a hydrogen (deuterium) pretreatment of the samples, was found to be related to the formation of hydrido (deutero) carbonyl clusters (experiment 6). These results suggest the occurrence of a direct interaction of hydrido species with gaseous CO_2, a mechanism that finds analogies with the CO_2 insertion reaction in M–H bonds of hydridocarbonyl complexes revealed in homogeneous conditions. These considerations are also supported by the examination of literature results reporting that (i) the key step in the CO_2 chemisorption on noble metal single crystals (the partial negative charge transfer from the metal to CO_2) is enhanced by lowering the work function of the metal; (ii) the work function of the noble metal single crystals is enhanced by hydrogen chemisorption.

(c) Study of the interactions between gaseous CO_2 and Rh/MgO and Rh/Al_2O_3, previously heated in a flowing oxygen stream, revealed that carbonyl clusters could be formed at temperatures higher than 200 °C by switching the CO_2 with helium; the carbonyl clusters decomposed if CO_2 was readmitted into the cell. These unusual reactivity features were tentatively explained as the result of a delicate balance between the temperature-induced aggregation reactions and the CO_2-induced oxidative and disaggregative reactions (experiment 7).

(d) A new cycle of reactions was revealed on the CeO_2 surface (see eqs 3 and 4); during this cycle the $Rh^I(CO)_2$ species were transformed into highly oxidized carbonyl complexes which were transformed again into $Rh^I(CO)_2$ species under a hydrogen environment. The same reactions were not obtained on MgO and Al_2O_3 surfaces (experiment 3).

(e) During the CO_2 methanation reaction the formation of only few kinds of clusters was strongly suggested by the features of the carbonyl stretchings which were enhanced in intensity, sharpened, and downward shifted at increasing temperatures between 50 and 300 °C. Broad bands assigned to geminal-, linear-, and bridge-bonded CO groups were revealed during CO methanation. This suggests that many different rhodium species are formed during CO hydrogenation. We have also found that when $Rh^I(CO)_2$ was the only species formed the hydrogenation of CO did not occur (experiments 4 and 8).

In addition to these new aspects of the rhodium chemistry, some previously described reactivity features were also confirmed. Their description had never been revealed under the conditions investigated here; in addition, all the reactivity features revealed in this study are useful for characterizing the solid materials to compensate the lack of structural information on the rhodium surface species.

Registry No. MgO, 1309-48-4; Al_2O_3, 1344-28-1; CeO_2, 1306-38-3; CO, 630-08-0; CO_2, 124-38-9; H_2, 1333-74-0.

References and Notes

(1) (a) Gates, B. C., Guczi, L., Knozinger, H., Eds. Metal clusters in catalysis. In *Studies in Surface Science and Catalysis*; Elsevier: Amsterdam, 1986; Vol. 29. (b) Lamb, H. H.; Gates, B. C.; Knozinger, H. *Angew. Chem., Int. Ed. Engl.* **1988**, *27*, 1127. (c) Basset, J-M., Gates, B. C., Candy, J. P., Choplin, A., Leconte, M., Quignard, F.; Santini, C. Eds. *Surface Organometallic Chemistry: Molecular Approaches to Surface Catalysis*; Kluwer: Dordrecht, 1988.

(2) Chini, P.; Heaton, B. T. In *Topics in Current Chemistry*; Springer-Verlag: Berlin, 1977; Vol. 71, pp 1–70 (and references therein).

(3) (a) Moser, W. R.; Chiang, C. C.; Thompson, R. W. *J. Catal.* **1989**, *115*, 532. (b) Basini, L.; Aragno, A.; Raffaelli, A. *J. Phys. Chem.* **1991**, *95*, 211. (c) Basini, L.; Patrini, R.; Aragno, A.; Gates, B. C. *J. Mol. Catal.* **1991**, *70*, 29.

(4) (a) Kubelka, P.; Munk, F. *Z. Z. Tech. Phys.* **1931**, *12*, 593. (b) Wendlands, W. W.; Hect, H. G. *Reflectance Spectroscopy*; Wiley: New York, 1966; pp 55–86. (c) Vincent, R. K.; Hunt, G. R. *Appl. Opt.* **1968**, *7*, 53.

(5) Chini, P.; Martinengo, S. *Inorg. Chim. Acta* **1969**, *3*, 315.

(6) (a) Yates, J. T., Jr.; Duncan, T. M.; Worley, S. D.; Waughan, R. W. *J. Chem. Phys.* **1979**, *70*, 1219. (b) Smith, A. K.; Hugues, F.; Theolier, A.; Basset, J-M.; Ugo, R.; Zanderighi, G-M.; Bilhou, J. L.; Bilhou-Bougnol, V.; Graidon, W. F. *Inorg. Chem.* **1979**, *18*, 3104. (c) Rice, C. A.; Worley, S. D.; Curtis, C. W.; Guin, J. A.; Tarrer, A. R. *J. Chem. Phys.* **1981**, *74*, 6487. (d) Yang, A. C.; Garland, C. W. *J. Phys. Chem.* **1957**, *61*, 1504.

(7) (a) Paul, D. K.; Yates, J. T., Jr. *J. Phys. Chem.* **1991**, *95*, 1699. (b) Paul, D. K.; Ballinger, T. H.; Yates, J. T., Jr. *J. Phys. Chem.* **1990**, *94*, 4617. (c) Ballinger, T. H.; Yates, J. T., Jr. *J. Phys. Chem.* **1991**, *95*, 1694. (d) Basu, T.; Panayotov, D.; Yates, J. T., Jr. *J. Am. Chem. Soc.* **1988**, *110*, 2074. (e) van't Blik, H. F.; van Zon, J. B. A.; Huizinga, T.; Konisberger, D. C.; Prins, R. *J. Phys. Chem.* **1985**, *89*, 4783.

(8) (a) Solymosi, F.; Knozinger, H. *J. Chem. Soc., Faraday Trans. 1* **1990**, *86*, 389. (b) Primet, M. *J. Chem. Soc., Faraday Trans. 1* **1978**, *74*, 2570.

(9) This hypothesis can not be substained by the unambiguous assignment of infrared bands to Rh–H stretchings (revealed by: Wey, J. P.; Neely, W. C.; Worley, S. D. *J. Phys. Chem.* **1991**, *95*, 8881) since these bands could not be distinguished, in the present case, from the carbonyl stretching bands.

(10) (a) Henderson, M. A.; Worley, S. D. *J. Phys. Chem.* **1985**, *89*, 392. (b) McKee, M. L.; Dai, C. H.; Worley, S. D. *J. Phys. Chem.* **1988**, *92*, 1056.

(11) (a) Wang, H. P.; Yates, J. T., Jr. *J. Catal.* **1984**, *89*, 79. (b) Kiss, J. T.; Gonzales, R. D. *J. Phys. Chem.* **1984**, *88*, 898. (c) Wey, J. P.; Neely, W. C.; Worley, S. D. *J. Catal.* **1992**, *134*, 378.

(12) (a) Li, C.; Sakata, Y.; Arai, T.; Domen, K.; Maruya, K.; Onishi, T. *J. Chem. Soc., Chem. Commun.* **1991**, 410. (b) Li, C.; Sakata, Y.; Arai, T.; Domen, K.; Maruya, K.; Onishi, T. *J. Chem. Soc., Faraday Trans. 1* **1989**, *85*, 929. (c) Jin, T.; Zhou, Y.; Mains, G. J.; White, J. M. *J. Phys. Chem.* **1987**, *91*, 5931. (d) Jin, T.; Zhou, Y.; Mains, G. J.; White, J. M. *J. Phys. Chem.* **1987**, *91*, 3310. (e) Breysse, M.; Guenin, M.; Claudel, B.; Latreille, H.; Veron, J. *J. Catal.* **1972**, *27*, 275. (f) Breysse, M.; Guenin, M.; Claudel, B.; Veron, J. *J. Catal.* **1973**, *28*, 54.

(13) The production of carbon-containing species through the dissociation of chemisorbed CO has already been revealed in with TPR experiments performed on supported transition-metal clusters, and these species are considered to be intermediates in the methanation and Fischer–Tropsch reactions.[14] The same dissociation reactions on rhodium single crystals are still a matter of controversy.[15]

(14) (a) Araki, M.; Ponec, V. *J. Catal.* **1976**, *44*, 439. (b) Ponec, V. *Catal. Rev.—Sci. Eng.* **1978**, *18*, 151. (c) McCarty, J. G.; Wise, H. *J. Catal.* **1979**, *57*, 406. (d) Goodman, D. W.; Kelly, R. D.; Madey, T. E.; Yates, J. T., Jr. *J. Catal.* **1980**, *63*, 226. (e) Bell, A. T. *Catal. Rev.—Sci. Eng.* **1981**, *23*, 23. (f) Biloen, P.; Sachtler, W. M. H. In *Advances in Catalysis*; Eley, D. D., Pines, H., Weisz, P. B., Eds.; Academic Press: New York, 1981; Vol. 30, pp 165–216. (g) Pebles, D. E.; Goodman, D. W.; White, J. M. *J. Phys. Chem.* **1983**, *87*, 4378. (h) Zagli, E.; Falconer, J. L. *J. Catal.* **1981**, *69*, 1. (j) Fujita, S.; Terunuma, H.; Nakamura, M.; Takezawa, N. *Ind. Eng. Chem. Res.* **1991**, *30*, 1146.

(15) (a) Castner, D. C.; Somorjai, G. A. *Surf. Sci.* **1979**, *83*, 60. (b) Yates, J. T., Jr., Williams, E. D.; Weinberg, W. H. *Surf. Sci.* **1980**, *91*, 562. (c) De Louise, L. A.; Winograd, N. *Surf. Sci.* **1984**, *138*, 417. (d) Marbrow, R. A.; Lambert, R. M. *Surf. Sci.* **1977**, *67*, 489. (e) Baird, R. J.; Ku, R. C.; Wynblatt, P. *Surf. Sci.* **1980**, *97*, 346. (f) Castner, D. G.; Sexton, B. A.; Somorjai, G. A. *Surf. Sci.* **1978**, *71*, 515. (g) Thiel, P. A.; Williams, R. D.; Yates, J. T., Jr.; Weinberg, W. H. *Surf. Sci.* **1979**, *84*, 54. (h) Kim, Y.; Pebles, D. E.; White, J. M. *Surf. Sci.* **1982**, *114*, 363. (i) Gurm, B. A.; Richter, L. J.; Villarubia, J. S.; Ho, W. *J. Chem. Phys.* **1987**, *87*, 6710. (l) Rebholz, M.; Prins, R.; Kruse, N. *Surf. Sci.* **1991**, *259*, L797.

(16) (a) Rosinek, M. P. *Catal. Rev.—Sci. Eng.* **1977**, *16*, 111. (b) Yao, J. C.; Yao, J. F. *J. Catal.* **1984**, *86*, 254. (c) Summers, J. C.; Ausen, S. *J. Catal.* **1979**, *58*, 131. (d) Rieck, T. S.; Bell, A. T. *J. Catal.* **1986**, *99*, 278.
(17) (a) Fischer, H. E.; Schwartz, J. *J. Am. Chem. Soc.* **1989**, *111*, 7644. (b) Cannon, K. C.; Jo, S. K.; White, J. H. *J. Am. Chem. Soc.* **1989**, *111*, 5064.
(18) Kung, M. C.; Kung, H. H. *Catal. Rev.—Sci. Eng.* **1985**, *27*, 425.
(19) (a) Solymosi, F.; Kiss, J. *Surf. Sci.* **1985**, *17*, 149. (b) Solymosi, F.; Kiss, J. *J. Chem. Phys. Lett.* **1984**, *110*, 639.
(20) (a) Henderson, M. A.; Worley, S. *J. Phys. Chem.* **1985**, *89*, 1417. (b) Solymosi, F.; Erdohely, A.; Bansagi, T. *J. Chem. Soc., Faraday Trans. 1* **1981**, *77*, 2645. (c) Solymosi, F.; Erdohely, A.; Bansagi, T. *J. Catal.* **1981**, *68*, 371. (d) Iizuka, T.; Tanaka, Y.; Tanabe, K. *J. Mol. Catal.* **1982**, *17*, 381. (e) Solymosi, F.; Pasztor, M. *J. Catal.* **1987**, *104*, 312. (f) Ichikawa, S. *Catal. Lett.* **1989**, *3*, 197. (g) Ichikawa, S. *J. Mol. Catal.* **1989**, *53*, 53.
(21) (a) Solymosi, F.; Bugyi, L. *J. Chem. Soc., Faraday Trans. 1* **1987**, *83*, 2015. (b) Kiss, J.; Renesn, K.; Solymosi, F. *Surf. Sci.* **1988**, *207*, 36. (c) Liu, Z. M.; Zhan, Y.; Solymosi, F.; White, J. M. *Surf. Sci.* **1981**, *245*, 289.
(22) (a) Mahan, G. D.; Lucas, A. A. *J. Chem. Phys.* **1979**, *68*, 1344. (b) Persson, B. N. J.; Ryberg, R. *Phys. Rev.* **1981**, *B24*, 6954. (c) Persson, B. N. J.; Liebisch, A. *Surf. Sci.* **1981**, *110*, 356. (d) Woodruff, D. P.; Heiden, B. E.; Prince, K.; Bradshaw, A. M. *Surf. Sci.* **1982**, *123*, 397. (e) Ueba, H. *Surf. Sci.* **1987**, *188*, 421.
(23) (a) Solymosi, F.; Erdohely, A. *J. Mol. Catal.* **1980**, *8*, 47. (b) Vannice, M. A. *J. Catal.* **1975**, *37*, 449. (c) Bardet, R.; Trambouze, Y. *C. R. Acad. Sci. Paris, Ser. C* **1979**, *288*, 101.
(24) (a) Biloen, P.; Sachtler, W. H. H. *Adv. Catal.* **1981**, *30*, 165. (b) Vannice, M. A. *Catal. Rev.—Sci. Eng.* **1976**, *14*, 153. (c) Bell, A. T. *Catal. Rev.—Sci. Eng.* **1981**, *23*, 203. (d) Mills, G. A.; Steffgen, F. W. *Catal. Rev.* **1978**, *10*, 139.
(25) (a) Weatherbee, G. D.; Bartholomew, C. H. *J. Catal.* **1981**, *67*. (b) Solymosi, F.; Erdohely, A.; Basagi, T. *J. Catal.* **1981**, *68*, 371. (c) Solymosi, F.; Erdohelyi, A.; Basagi, T. *J. Catal.* **1981**, *62*, 165.
(26) (a) Berkő, A.; Solymosi, F. *Surf. Sci.* **1987**, *187*, 359. (b) Liu, Z. M.; Zhou, Y.; Solymosi, F.; White, J. M. *Surf. Sci.* **1991**, *245*, 289. (c) Kiss, J.; Révész, K.; Solymosi, F. *Surf. Sci.* **1988**, *207*, 36. (d) Berkő, A.; Solymosi, F. *Surf. Sci. Lett.* **1986**, *171*, L498. (e) Solymosi, F. *J. Mol. Catal.* **1991**, *65*, 337.
(27) (a) Behm, R. J.; Christmann, K.; Ertl, G. *Surf. Sci.* **1990**, *99*, 320. (b) Behn, R. J.; Fenka, V.; Cattania, M. G.; Christmann, K.; Ertl, G. *J. Chem. Phys.* **1983**, *78*, 7486. (c) Solymosi, F.; Kovacs, I. *J. Phys. Chem.* **1989**, *93*, 7537. (d) Ehsasi, M.; Christmann, K. *Surf. Sci.* **1988**, *194*, 172. (e) Christmann, K.; Ehsasi, M.; Hirschwald, W.; Block, J. H. *Chem. Phys. Lett.* **1986**, *136*, 192. (f) Lauth, G.; Schvartz, E.; Christmann, K. *J. Chem. Phys.* **1989**, *91*, 3729.
(28) (a) Eisenberg, R.; Hendrikson. *Adv. Catal.* **1987**, *28*, 119. (b) Darensbourg, J.; Ovalles, C. *J. Am. Chem. Soc.* **1984**, *106*, 3750. (c) Pugh, J. R.; Bruce, M. R. M.; Sullivan, B. P.; Meyer, T. J. *Inorg. Chem.* **1991**, *30*, 86. (d) Braunstein, P.; Hatt, D.; Nobel, D. *Chem. Rev.* **1988**, *88*, 747. (e) Darensbourg, D. J.; Wiengreffe, H. P.; Wiengreffe, P. W. *J. Am. Chem. Soc.* **1990**, *112*, 9252. (f) Darensbourg, D. J.; Kudaroski, R. *Adv. Organomet. Chem.* **1983**, *22*, 129. (g) Palmer, D. A.; van Eldik, R. *Chem. Rev.* **1983**, *83*, 651.

Heterogeneous Chemistry of HBr and HF

David R. Hanson* and A. R. Ravishankara

NOAA Aeronomy Lab, 325 Broadway, Boulder, Colorado 80303, and Cooperative Institute for Research in Environmental Sciences University of Colorado, Boulder, Colorado 80309 *(Received: May 21, 1992; In Final Form: August 19, 1992)*

The heterogeneous chemistry of HBr and HF was studied on glass and ice surfaces at 200 K. Physical and reactive uptake were investigated using a cylindrical fast-flow reactor in conjunction with a chemical-ionization mass spectrometer. HF exhibited no measurable uptake on ice or NAT nor did it significantly react with $ClONO_2$ or HOCl. It is inferred that HF would be unreactive on polar stratospheric cloud particle surfaces. Physical adsorption or absorption of HBr was observed onto glass, adsorbed H_2O layers on glass, and ice. For the relatively high [HBr] used, a very large uptake by ice was observed, and we detected no saturation of the surface. HBr reacts efficiently with $ClONO_2$, Cl_2, and N_2O_5, especially on ice and nitric acid ice surfaces. BrCl was observed as the primary product for the reaction HBr + $ClONO_2$. The products HCl and Br_2 were observed for the reaction of HBr with Cl_2. On the basis of these results, it is likely that HBr would be processed efficiently on ice particles.

Introduction

The heterogeneous processing of reservoir chlorine species, mainly HCl and $ClONO_2$, into easily photolyzed forms is essential for the occurrence of the Antarctic ozone hole.[1] The heterogeneous chemistry of HCl has recently come under extensive investigation[2-10] and reactions of HOCl and $ClONO_2$ with HCl adsorbed on the surface of ice were found to be very efficient.[9,10] The bromine analogues of the chlorine reservoirs, HBr and $BrONO_2$, are short lived due to rapid gas-phase processes.[11] Yet, it is of interest to study the possible heterogeneous reactions of these species. Heterogeneous processes may be especially important when gas-phase processing is slow such as during the polar night. In addition, heterogeneous processing of bromine compounds may play a role in the rapid loss of ozone observed in the winter arctic troposphere.[12]

Heterogeneous processing of HF would have a large impact on its chemistry and its use as a tracer, as it is currently thought to be inert.[13] It is believed that the majority of fluorine released in the degradation of fluorocarbon molecules ends up as HF. At present, stratospheric levels of HF are comparable to HCl, especially in the Antarctic stratosphere. The abundance of HF is expected to increase or remain high as the current CFCs (chlorofluorocarbons) are replaced with compounds that contain less chlorine and in many cases, more fluorine.[14] The gas-phase reaction of HF with $ClONO_2$ is endothermic, unlike the case of HCl + $ClONO_2$. Yet HF may react on the surface of a particle via dissociation of HF or $ClONO_2$ on the surface. Therefore, it is important to know if reactions such as HF + $ClONO_2$ can occur heterogeneously and if so, how efficiently.

This is the first investigation of the heterogeneous reactions of HBr and HF. The primary aim of this work was to qualitatively assess if such processes can occur and, if they do take place, their importance in the atmosphere. Therefore, mechanistic information was the major goal. Quantitative loss rate parameters were determined only when the process was determined to be important and also experimentally feasible.

Our first step in assessing the heterogeneous reactivities of HBr and HF was to study their physical uptake onto water ice near 200 K. We are aware of no studies of this kind for HBr or HF. The physical uptake of HCl by ice has been investigated by a number of researchers (refs 9 and 10 and references therein) and the uptake phenomena reported for HCl help us interpret our measurements for HBr and HF by ice surfaces.

To investigate the reactivity of HBr and HF, we studied the reactions of $ClONO_2$ with HBr and HF on ice. In addition, the reactions of HBr with Cl_2 and N_2O_5 were explored. We also performed some experiments over a cold glass surface for reactions involving the HBr molecule. In some of these experiments, water

0022-3654/92/2096-9441$03.00/0